8

NMR AND EPR INVESTIGATIONS OF BI-METALLOENZYMES

J. J. VILLAFRANCA[†] and F. M. RAUSHEL[††]

[†]Department of Chemistry
The Pennsylvania State University
University Park, PA 16802

and

[††]Department of Chemistry
Texas A&M University
College Station, TX 77840

I. INTRODUCTION

Many enzymes that catalyze a wide range of different chemical reactions utilize cations as part of the structure and/or catalytic sites of the enzyme. In this manuscript we will discuss two classes of enzyme: 1) enzymes that require

two divalent cations for activity and 2) enzymes that require a monovalent and a divalent cation for activity. In this latter category Suelter (1) described several classes of enzymes that were activated by monovalent cations. He concluded that a common theme existed among them, namely, reactions in which a keto-enol tautomerization was a likely event. The role of the monovalent cation in these reactions was supposedly to stabilize the enolate anion for further reaction through this species. This attractive idea suffers from lack of experimental proof to verify enzyme-bound enolate-cation species.

Within this class of enzymes that are activated by monovalent cations are several which catalyze phosphoryl transfer reactions. Perhaps the best studied is pyruvate kinase, whose reaction is given below.

$$\text{ATP + Pyruvate} \xrightleftharpoons{M^{2+},M^{+}} \text{ADP + Phosphoenolpyruvate (PEP)} \qquad (1)$$

In fact, two divalent cations are required, one structural and the other bound to ATP (2). The role of the monovalent cation is less clear. Upon substitution of Mn^{2+} for the physiologically important Mg^{2+} in this reaction, a paramagnetic probe is introduced at the active site of the enzyme and several structural experiments can be conducted. NMR studies of the paramagnetic influence of Mn^{2+} on relaxation rates of several substrate nuclei permit calculation of distances among these nuclei (3). This approach can also be applied to measure the distance between the monovalent and divalent cation sites and it is this application which was studied in our laboratory.

II. PROPERTIES OF MONOVALENT CATIONS

Table I lists monovalent cations of the alkali metal series and also Tl^{+}. All are observable by NMR spectroscopy and all but Tl^{+} have a nuclear spin greater than 1/2. Those nuclei with $S > 1/2$ possess a quadrupolar moment, Q, which affects their relaxation properties and hence their applicability for high resolution NMR studies with enzymes. The table gives the quadrupole moment of each nucleus, its natural abundance, and NMR sensitivity relative to the natural abundance of ^{13}C (1.1%) to provide a benchmark for comparison. The only practical way to study ^{6}Li is to obtain it in enriched form from a government laboratory such as Oak Ridge. An important point to consider from examination of this table is that all nuclei are quite easily observed in standard multinuclear NMR spectrometers at reasonable concentrations, 1-100 mM (with the possible exception of ^{39}K and assuming enriched ^{6}Li is used).

Table I also presents the line widths obtained for dilute samples of each of these ions. An equation describing the factors that contribute to the line

TABLE I

NMR PROPERTIES OF MONOVALENT CATIONS[a]

Nucleus	Spin	Q	% Natural Abundance	NMR Sensitivity (^{13}C = 1)	Line Width Hz, 25 °C
^{6}Li	1	0.00046	7.42	3.58	.002
^{7}Li	3/2	-0.042	92.58[b]	1540	.01
^{23}Na	3/2	0.11	100	525	4.5
^{39}K	3/2	0.055	93.08	2.69	4.8
^{85}Rb	5/2	0.247	72.15	43	130
^{87}Rb	3/2	0.12	27.85	277	140
^{133}Cs	7/2	-0.003	100	269	.02
^{205}Tl	1/2	-	70.5	769	.30

[a]Data from reference (5).
[b]U.S. Government removes the ^{6}Li.

width is given below:

$$\text{Line width (Hz)} \propto \frac{1}{T_2} \propto \frac{2I+3}{I^2(2I-1)} \cdot Q^2 \cdot A^2 \qquad (2)$$

Equation 2 is from a theoretical treatment by Hertz (4) and is presented here in simplified form to stress the factors that contribute to the line width of a quadrupolar nucleus. Q is the aforementioned quadrupole moment. This value enters the equation as the square and an increase in Q contributes significantly to the overall line width. The expression for I, the nuclear spin, actually predicts that the line width will be narrower the larger this value becomes. This is contrary to most expectations. The term that contributes most significantly in eq 2, however, is A, the Sternheimer antishielding factor. A thorough list of these values can be found in a chapter by Lindman and Forsén (5) but two examples will be given here.

Both ^{7}Li and ^{85}Rb have I = 3/2, but the line widths of these two cations differ by $\sim 10^4$. The difference in Q accounts for only a factor of $\sim$35 in the line width. The critical difference is the Sternheimer antishielding factor which has values of $\sim$0.74 for $^{7}Li^+$ and $\sim$48 for $^{85}Rb^+$. This factor alone accounts almost totally for the difference in line width. The trend is that the Sternheimer antishielding factor increases as one goes down a column of the periodic table. The narrow line width for $^{133}Cs^+$ arises from a small value of Q and a large I which offsets a large value of A (111 for $^{133}Cs^+$).

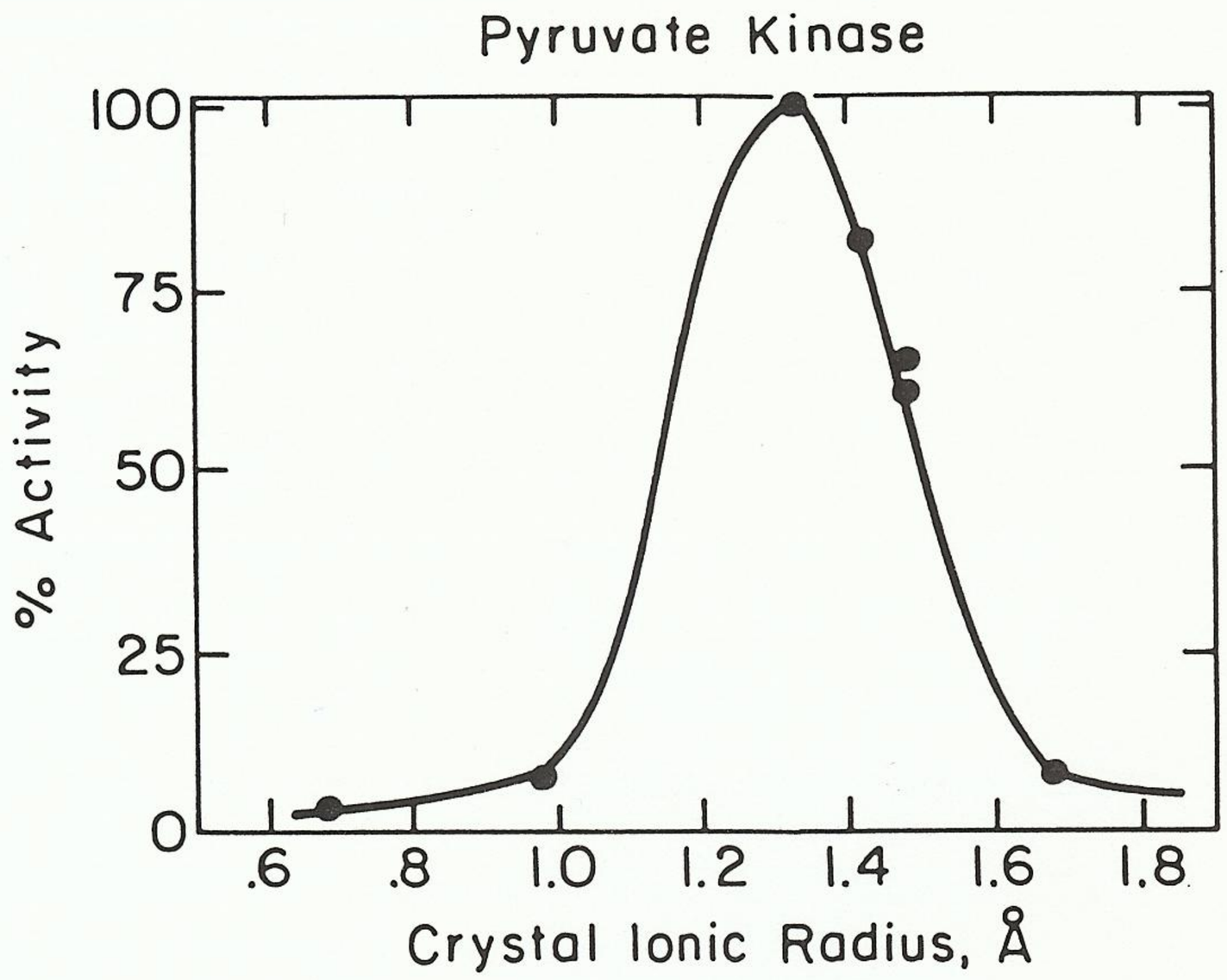

Fig. 1. Correlation of percent activity of pyruvate kinase versus crystal ionic radius of various monovalent cations.

A. Pyruvate Kinase

Several studies have been conducted to determine how the specific activity of pyruvate kinase varies as a function of monovalent cation concentration. Kayne (6) determined that K^+ stimulates pyruvate kinase to the greatest extent, whereas ions like Li^+ and Cs^+ were less active. Figure 1 shows a correlation of % activity with crystal ionic radius for Li^+ (0.68 Å), Na^+ (0.97 Å), K^+ (1.33 Å), NH_4^+ (1.43 Å), Rb^+ (1.47 Å), Tl^+ (1.47 Å), and Cs^+ (1.67 Å). Nowak (7,8) has made a systematic study of mono-, di-, tri-, and tetramethylammonium ion as activators of pyruvate kinase and has shown that only monomethylammonium ion activates (∿0.5 % relative to K^+). These ions would be expected to be poor activators due to the bulky methyl substituent on nitrogen.

NMR measurements of the longitudinal relaxation rates ($1/T_1$) of monovalent cations present an opportunity to correlate structural data on pyruvate kinase with data on the activity produced by each monovalent cation site relative to the sites for the other ligands of pyruvate kinase, a number of laboratories have used NMR to measure the distance from enzyme-bound Mn^{2+} to the monovalent cation site. This metal ion site is the structural site, not the metal-nucleotide site. Reuben and Kayne (9) have reported distances of 4.9 and 8.2 Å between $^{205}Tl^+$ and Mn^{2+} in the enzyme-Mn^{2+}-Tl^+-PEP complex and the enzyme-Mn^{2+}-Tl^+

complex, respectively. In a ^{7}Li-NMR study, Hutton et al. (10) reported distances of 5.8 and 11.0 Å for these enzyme-Mn^{2+} complexes with $^{7}Li^{+}$. Since Li^{+} activates only 3% as well as Tl^{+}, these authors proposed that the longer metal-metal distance for the Li^{+} complexes compared with the Tl^{+} complexes correlated with the large decrease in enzymatic activity. Ash et al. (11) pointed out that there are two interconvertible forms of the enzyme-Mn^{2+}-Li^{+}-PEP (12) which Hutton at al. did not allow for. Repeating the ^{7}Li-NMR experiments, Ash et al. obtained distances between between Mn^{2+} and Li^{+} that are nearly identical with the Mn^{2+}-Tl^{+} distances of Reuben and Kayne. However, the choice of a correlation time (τ_c) for the dipolar Mn^{2+}-Li^{+} interaction explains the difference in the measured distances in these two ^{7}Li-NMR studies. Hutton et al. used a value of 9.4 ns, while Ash et al. used a value of 1.7 ns. This latter value was obtained from a study of water proton relaxation rates. Nowak found distances between Mn^{2+} and the methyl protons of mono-, di-, tri-, and tetramethylammonium ion of 6.5 Å, 7.8 Å, 8.7 Å, and 10.9 Å, respectively, in enzyme complexes with PEP (8).

We expanded the list of monovalent cations studied for pyruvate kinase by NMR to include $^{6}Li^{+}$, $^{7}Li^{+}$, $^{14}NH_4^{+}$, $^{15}NH_4^{+}$, $^{23}Na^{+}$, $^{39}K^{+}$, $^{85}Rb^{+}$, $^{87}Rb^{+}$, and $^{133}Cs^{+}$ (13). Spin-lattice relaxation times (T_1) for the various monovalent cations were determined using a 180°-τ-90° pulse sequence with a 200 MHz NMR spectrometer. A few experiments with $^{15}NH_4^{+}$ and $^{7}Li^{+}$ were also performed with 100 and 360 MHz spectrometers. The values for the spin-lattice relaxation times of the various monovalent cations in different solutions at 30 °C are shown in Table II. Table II reveals substantial effects on the spin-lattice relaxation

TABLE II

NMR DATA FOR VARIOUS MONOVALENT CATIONS[a]

Nucleus	Frequency (MHz)	T_1 Values			
		Buffer	Mg^{2+}-PEP-enzyme	Mn^{2+}-PEP-enzyme	Mn^{2+}-enzyme
$^{6}Li^{+}$	29	151	93	2.0	17
$^{7}Li^{+}$	78	15.1	10.8	0.79	4.4
$^{133}Cs^{+}$	26	10.3	7.4	2.1	4.5
$^{14}NH_4^{+}$	14	0.51	0.52	0.32	0.41
$^{15}NH_4^{+}$	10	42	41	0.53	6.8
$^{23}Na^{+}$	53	0.043	0.041	0.040	0.041
$^{39}K^{+}$	9	0.037	0.022	0.018	-
$^{87}Rb^{+}$	65	0.0018	0.0017	0.0017	-

[a]Data from reference 13.

times of $^{6}Li^{+}$, $^{7}Li^{+}$, and $^{14}NH_4^{+}$ (100 mM solutions of these ions). In agreement with the results of Reuben and Kayne (9), Ash at al. (11) and Hutton et al. (10), there is a substantially larger effect on the T_1 values in the enzyme-Mn^{2+}-M^{+}-PEP complex than in the enzyme-Mn^{2+}-M^{+} complex. This is consistent with PEP causing the Mn^{2+}-M^{+} distance to shorten significantly.

The data in Table II can be used to compute distances between Mn^{2+} and the various monovalent cations. However, a problem in using NMR data to compute internuclear distances between paramagnetic centers and ligands bound to a macromolecule is the determination of the correlation time, τ_c, for the electron-nuclear interaction (14). Practice has shown that the dipolar electron-nuclear interaction dominates the relaxation processes for several paramagnetic species and that relaxation can be described by the Solomon-Bloembergen equation (14). The simplified form of this equation applicable to longitudinal relaxation data obtained with paramagnetic centers and $\tau_c \geq 10^{-10}$s is given by eq 3.

$$r = C \left[T_{1M} \cdot \frac{3\tau_c}{(1 + \omega_I^2 \tau_c^2)} \right]^{1/6} \qquad (3)$$

In this equation, r is the electron-nuclear distance, C is a collection of constants whose value depends on the spin of the paramagnetic center and the gyromagnetic ratio of the nucleus, T_{1M} is the spin-lattice relaxation time attributable to the influence of the paramagnetic species, and ω_I is the nuclear Larmor precession frequency. This treatment also assumes fast exchange conditions and therefore that $1/T_{1p} = 1/T_{1M}$, in which $1/T_{1p}$ is the observed relaxation rate corrected for diamagnetic effects.

Several methods have been described to estimate a value of τ_c for use in calculating distances: A) measurement of T_1 and T_2 values for the nuclei, B) a frequency dependence of T_1 of the nuclei, C) a frequency dependence of the relaxation rates of solvent water in the system, and D) measurement of the line width of the EPR spectrum of the paramagnetic species. Of these, B) gives the best results but, of course, requires that data be obtained using two spectrometers. Also for some ions, e.g., Mn^{2+} and Cu^{2+}, the relevant correlation time for the dipolar relaxation is the electron spin relaxation time, which itself can be magnetic field dependent, further complicating the data analysis.

It occurred to us that an unambiguous determination of the correlation time could be made by performing identical experiments with $^{6}Li^{+}$ and $^{7}Li^{+}$ at the same magnetic field strength, thus obviating many of the problems discussed above (15). From the ratio of the observed T_{1p} (T_{1M}) values for $^{6}Li^{+}$ and $^{7}Li^{+}$ a

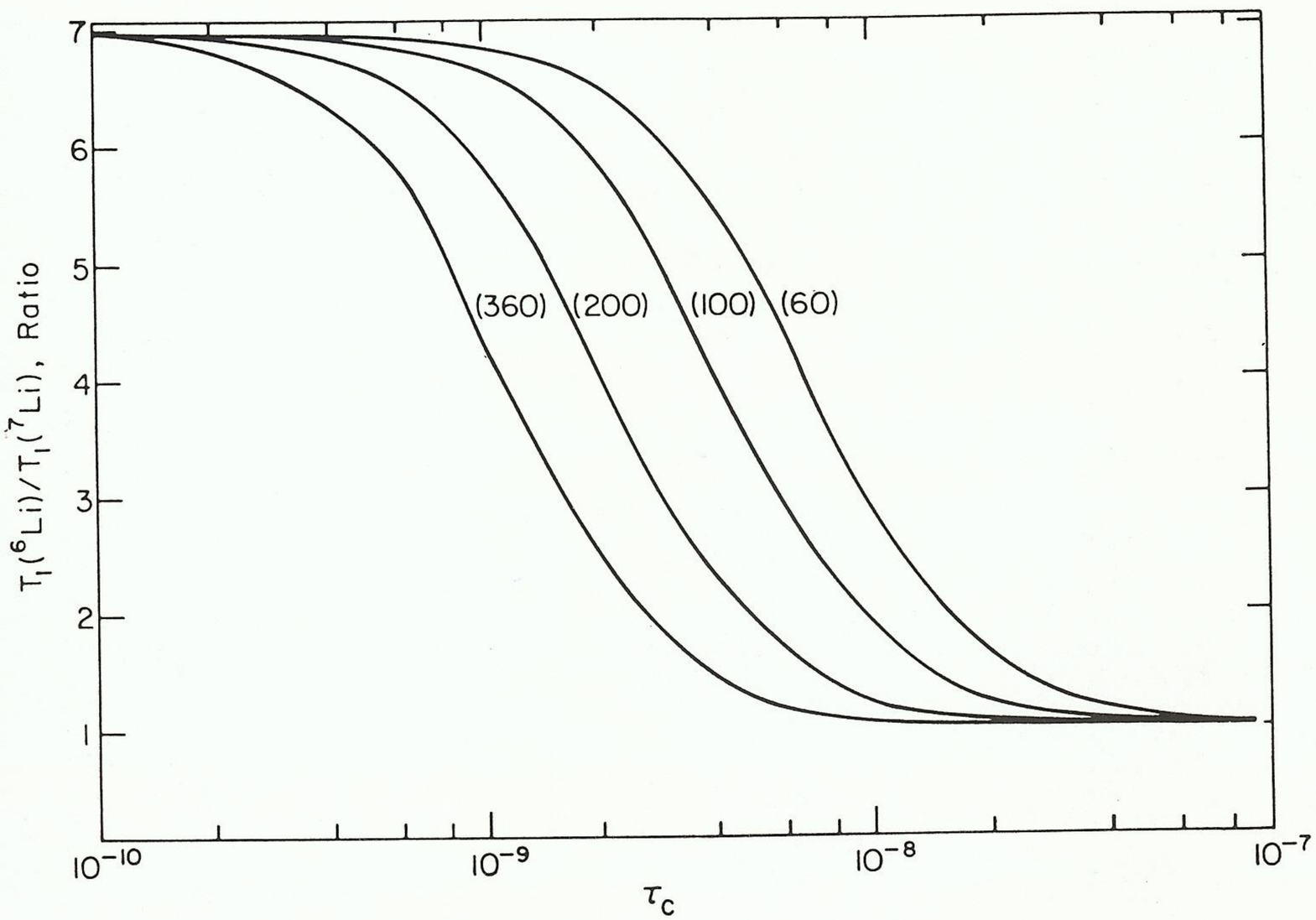

Fig. 2. Plot of the ratio of T_{1M} values for ^6Li and ^7Li versus correlation time. This plot derives from equation 3. The curves correspond to various magnetic field strengths, with the frequency in MHz for ^1H at each field strength given on the curves for ease of identification.

unique value of τ_c is obtained because in equation 3, C and ω_I are known values for the two isotopes of lithium, and the distance r must be the same for both ions. Examination of theoretical plots (Figure 2) of the ratio of T_{1M} values for $^6Li^+$ and $^7Li^+$ at various magnetic field strengths versus a range of correlation times commonly found in enzyme-Mn^{2+} complexes shows that this method is very sensitive for the determination of τ_c values of $<10^{-8}$s, since in this range the T_{1M} values for $^6Li^+$ and $^7Li^+$ are quite different. The ratio of these T_{1M} values changes from $\sim$1 to $\sim$7 at all field strengths. Similar plots can also be constructed for the two isotopes of NH_4^+ (^{15}N and ^{14}N) (Figure 3) and for Rb^+ (^{87}Rb and ^{85}Rb) (not shown).

Using the data in Table II, the $1/T_{1M}$ values for the PEP-Mn^{2+}-enzyme complexes of $^6Li^+$ and $^7Li^+$ are 1.21×10^3 and 2.89×10^3 s^{-1}, respectively. From this ratio and equation 3 for each isotope, a τ_c of 3.7×10^{-9}s is calculated. Also, using the relaxation data for $^7Li^+$ obtained at 78 and 39 MHz (Table II) and the

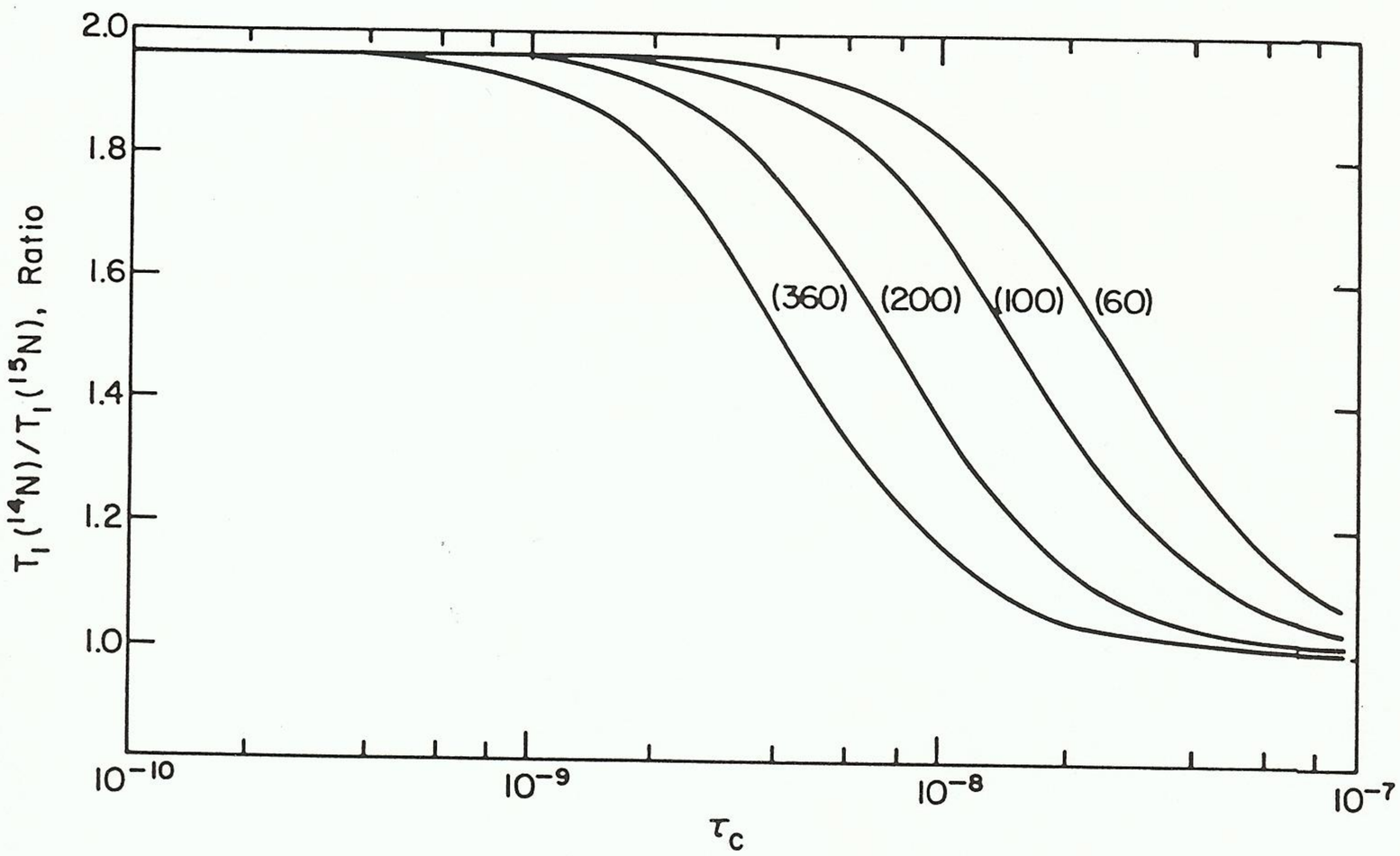

Fig. 3. Plot of the ratio of T_{1M} values for ^{14}N and ^{15}N versus correlation time. Same conditions as for Figure 2.

TABLE III

DISTANCES BETWEEN Mn^{2+} AND MONOVALENT CATIONS

Monovalent Cation	$E\text{-}Mn^{2+}\text{-}M^{+}$ Distance (Å) no PEP	$E\text{-}Mn^{2+}\text{-}M^{+}$ Distance (Å) with PEP
Li^{+} [a]	8.4 ± 0.4	5.7 ± 0.3
Na^{+} [a]	-	≥4.5
Cs^{+} [a]	7.7 ± 0.4	6.0 ± 0.3
Rb^{+} [a]	-	≥4.1
NH_4^{+} [a]	7.0 ± 0.4	4.4 ± 0.3
K^{+} [a]	-	≥3.7
Tl^{+} [b]	8.2 ± 0.5	4.8 ± 0.3
$CH_3NH_3^{+}$ [c]	8.7 ± 0.5	6.5 ± 0.3

[a] From reference (13).
[b] From reference (9).
[c] From reference (8).

data of Hutton et al. at 24 MHz, a τ_c value of 3.4×10^{-9}s was obtained from the ratio of the slope to intercept in a plot of T_{1M} versus ω_1^2 (16).

Table III shows that reliable distances between Mn^{2+} and the monovalent cations were obtained from the present data for Li^+, NH_4^+, and Cs^+ while only lower limits for the distances to Na^+, K^+, and Rb^+ were obtained. There are two general observations to be made from the data in Table III. The first is that there is a 2-3 Å change in the distance between Mn^{2+} and all of the monovalent cations when PEP is added to the system. This is consistent with previous data. The second observation is that the cations that are better activators of the enzyme are also significantly closer to the Mn^{2+} in the complex with PEP than are the poorer activators. NH_4^+ and Tl^+ are 4.4-4.8 Å away, while Li^+ and Cs^+ are 5.8-6.0 Å away. This suggests that the orientation of ligands on pyruvate kinase in the presence of the good monovalent activators is significantly different than it is in the presence of the poor monovalent cation activators. Previous data by Nowak on monomethylammonium cation are also consistent with this idea since this cation produces about 0.5% of the activity of K^+ and is 6.5 Å from Mn^{2+}. Figure 4 presents the results of the distance determinations thus far, and a reasonable correlation between percent activity and Mn^{2+}-M^+ distance is demonstrated. Just how this metal-ion-induced structure change between

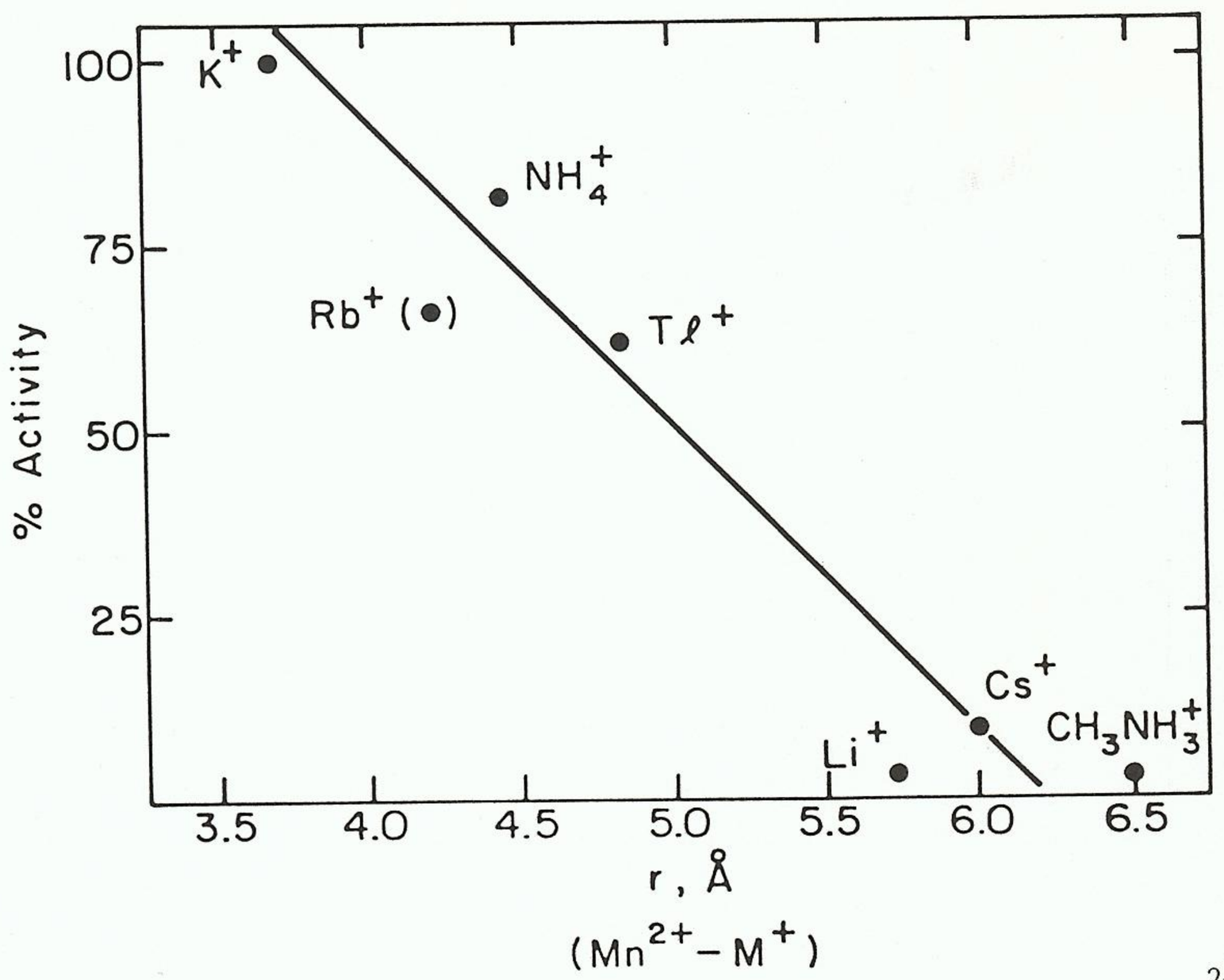

Fig. 4. Correlation of percent activity of pyruvate kinase versus Mn^{2+} to monovalent cation distance derived from the NMR data.

metal ion sites alters the orientation of substrates at the active site is still unknown.

B. Carbamoyl-Phosphate Synthetase

Experiments have just been initiated in our laboratory on structural studies of carbamoyl-phosphate synthetase from E. coli. The reaction catalyzed by this enzyme is given below.

$$2ATP + HCO_3^- + \text{glutamine} \xrightarrow{M^{2+},M^+} 2ADP + P_i + \text{carbamoyl-P} + \text{glutamate} \quad (4)$$

Recent work from our laboratory established that there is a structural site for divalent cations as well as the two metal ATP sites (16). In addition, a monovalent cation is required for activity.

Using an approach similar to that described for pyruvate kinase, we studied the effect of Mn^{2+} (bound at the structural metal ion site) on the longitudinal relaxation rates of $^6Li^+$, $^7Li^+$, and $^{15}NH_4^+$ (17). From these experiments the $1/T_{1M}$ values in s^{-1} were 620 ($^7Li^+$), 170 ($^6Li^+$), and 170 ($^{15}NH_4^+$), respectively. From the ratio of $1/T_{1M}$ values for ^6Li and ^7Li, a τ_c value of 3.2×10^{-9} s was obtained. Distances from Mn^{2+} to M^+ calculated using eq 3 were 7.6 ± 0.4 Å (Mn^{2+} to Li^+) and 7.4 ± 0.5 (Mn^{2+} to NH_4^+). Further correlations of structure-reactivity parameters with this enzyme are underway to assess the influence of substrates and allosteric modifiers on the Mn^{2+}-M^+ distance.

C. General Applicability of the NMR Method

One can evaluate the general applicability of the NMR method to calculate metal-metal distances in enzyme systems by computing a theoretical plot of "maximum distance" for each of the monovalent cations discussed in this chapter. Using Mn^{2+} as our paramagnetic probe, a practical upper limit for a Mn^{2+}-M^+ distance can be computed using the following reasonable assumptions: 1) a change in T_1 of the monovalent cations of 33% was observed between enzyme-Mg^{2+} and enzyme-Mn^{2+}, and 2) a reasonable ratio of free-to-bound monovalent cation could be achieved experimentally. This ratio depends upon the binding constant for M^+ for each cation. Figure 5 shows a theoretical plot (using eq 3) of "maximum distance" as a function of correlation time over a wide range of τ_c values. For this plot, a magnetic field of 47 Kgauss was chosen (for use in eq 3).

The monovalent cations fall into roughly three groups from this theoretical analysis. $^6Li^+$, $^7Li^+$, $^{15}NH_4^+$, and $^{133}Cs^+$ can be used to measure distances from 12-20 Å with reasonable accuracy. $^{14}NH_4^+$, $^{205}Tl^+$, and $^{23}Na^+$ are useful only for

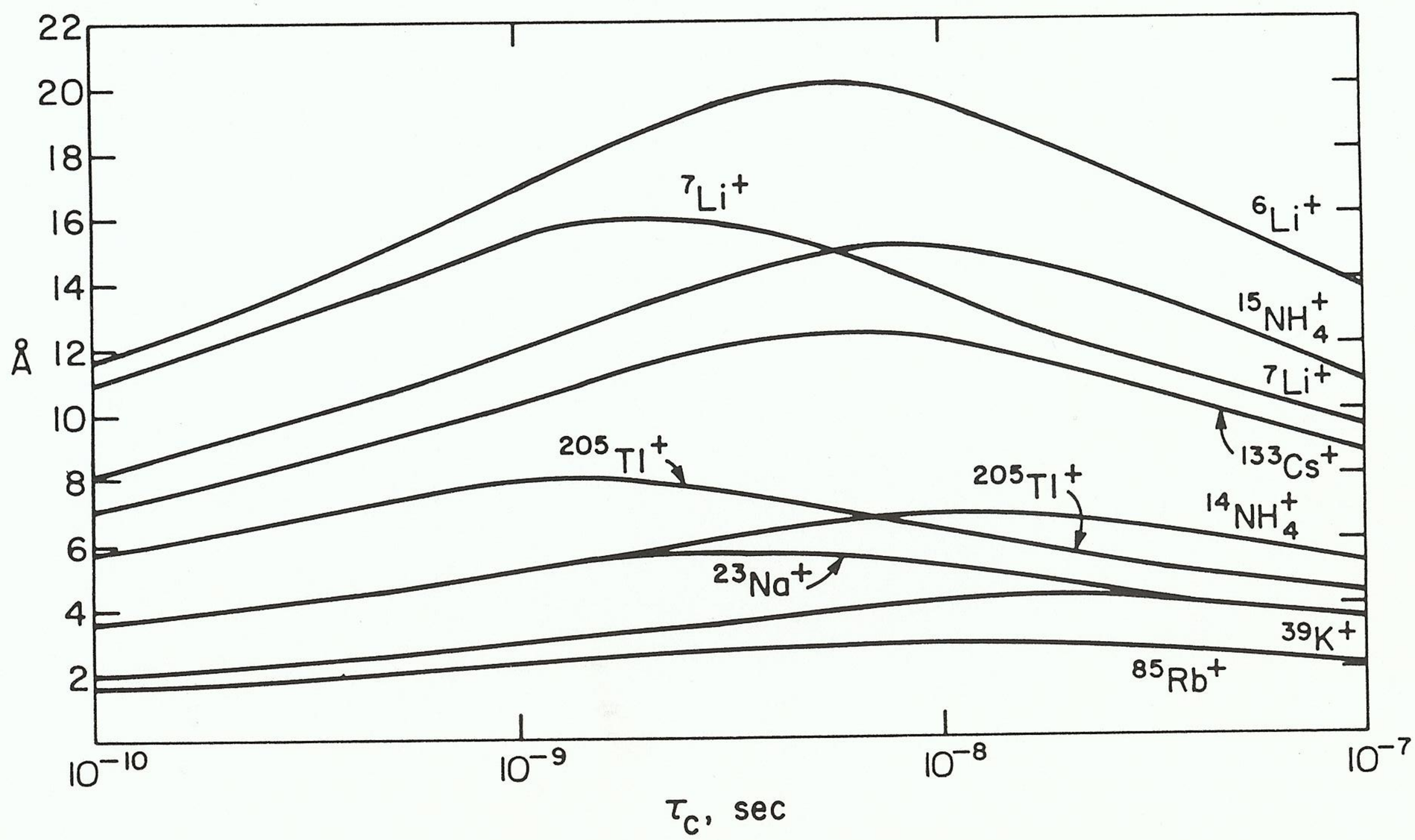

Fig. 5. Plot of "maximum distance" from Mn^{2+} to various monovalent cations versus correlation time. Details are given in the text for the calculations based on equation 3.

shorter distances in the range 4 - 8 Å, whereas $^{39}K^{+}$, ^{85}Rb, and $^{87}Rb^{+}$ are useful for distances ≤4 Å. Another parameter which can influence the distance determination is choice of magnetic field strength. The same theoretical calculation as that shown in Figure 5, but for 23 Kgauss magnetic field strength, indicates that longer distances can be measured by decreasing the strength of

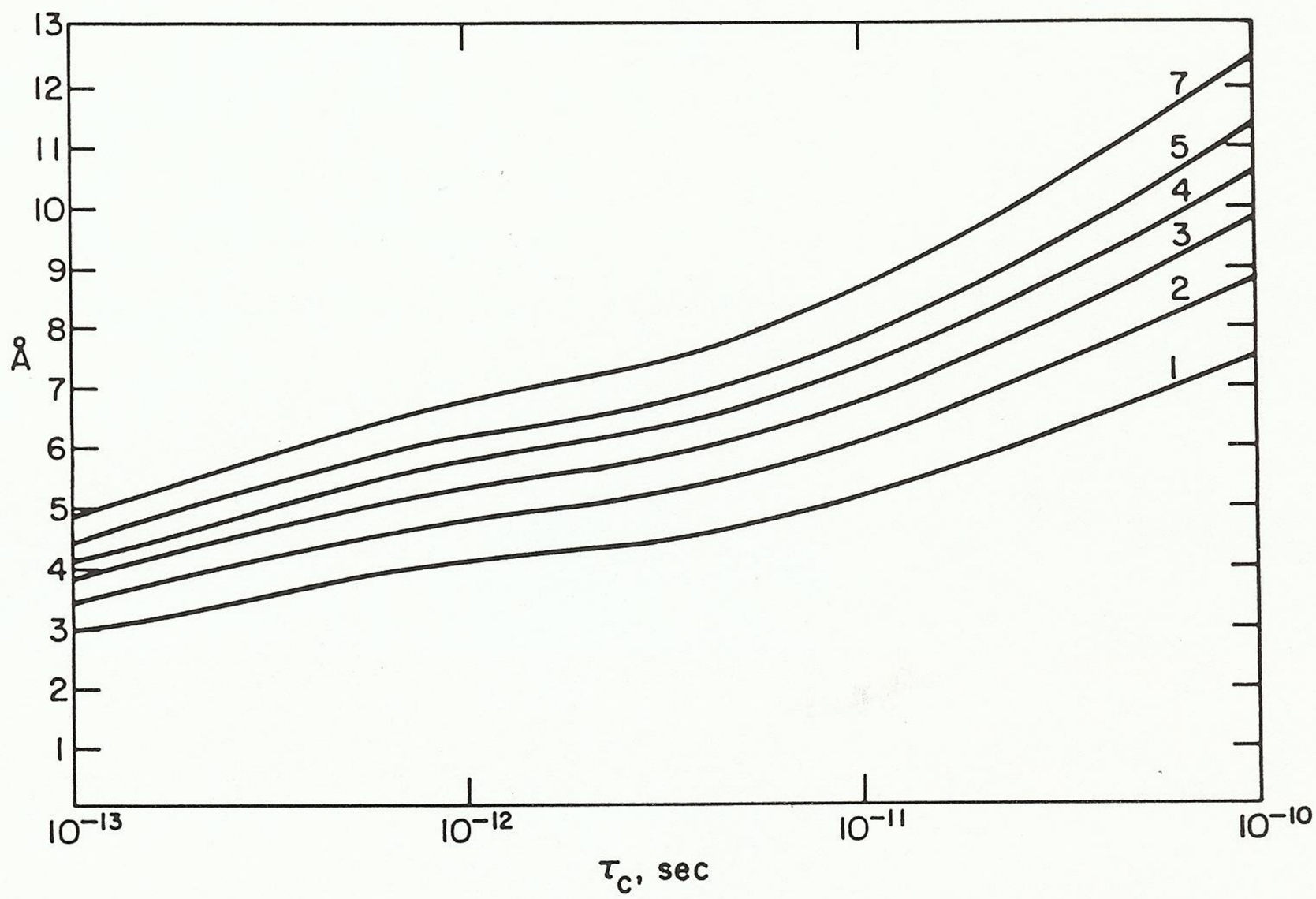

Fig. 6. Plot of "maximum distance" for ^{6}Li with various paramagnetic species. The numbers next to the curves correspond to the number of unpaired electrons. For all systems g is assumed to be 2.0 for simplification, and the magnetic field strength is 47 Kgauss. Correlation times are from 10^{-13} to 10^{-10}s.

the field since greater paramagnetic effects are seen with Mn^{2+} under these conditions.

If paramagnetic species other than Mn^{2+} are bound to an enzyme, this method is useful, but the paramagnetic effect obviously changes with the number of electrons and thus the "maximum distance" changes. Figures 6 and 7 show the "maximum distance" for $^{6}Li^{+}$ interacting with 1, 2,3, 4, 5, and 7 unpaired electrons (following the S(S+1) selection rules) as a function of correlation time covering the range 10^{-7} to 10^{-13}s. One can obtain an "estimate" of distance and thus

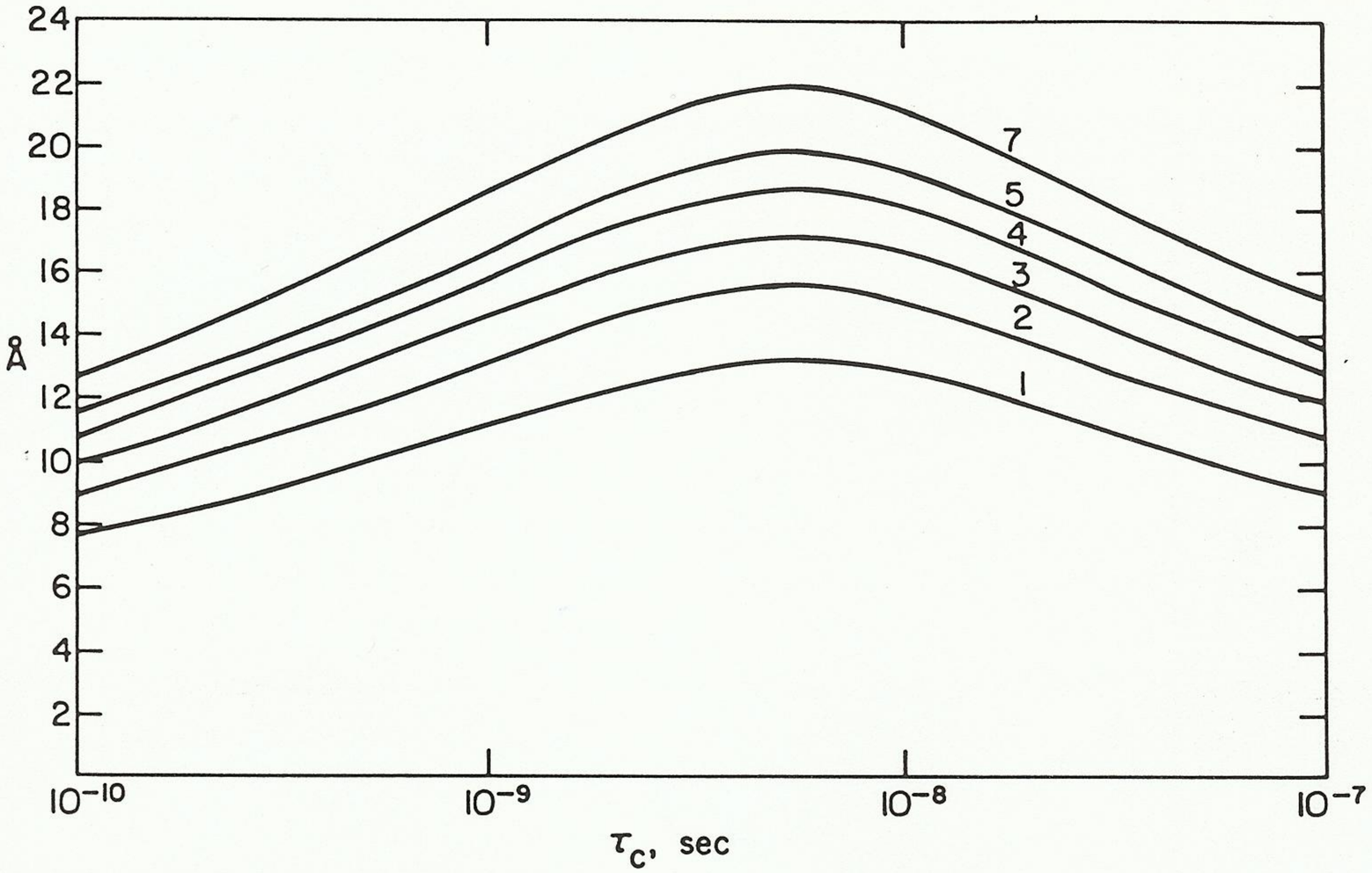

Fig. 7. Same plot as in Figure 6 but in the range of correlation times from 10^{-10} to 10^{-7}s.

the feasibility of an experiment if one consults Table IV, in conjunction with Figures 6 and 7, for the range of correlation times for various paramagnetic species that could be bound to an enzyme. It can be seen that the method is useful for many different systems.

TABLE IV

τ_s VALUES FOR SEVERAL PARAMAGNETIC SPECIES

Number of Unpaired Electrons	Paramagnetic species	τ_s Range (s)
7	Gd^{3+}	10^{-9} to 10^{-10}
5	Mn^{2+}	10^{-9} to 10^{-8}
1	Cu^{2+}	$\sim 5 \times 10^{-10}$ to $\sim 5 \times 10^{-9}$
5	Fe^{3+} (high-spin)	10^{-11} to 10^{-9}
1	Fe^{3+} (low-spin)	$\sim 10^{-11}$
3	Co^{2+} (high-spin)	$\sim 5 \times 10^{-13}$ to 10^{-11}
2	Ni^{2+} (high-spin)	$\sim 10^{-12}$
4	Fe^{2+} (high-spin)	$\sim 10^{-12}$
3	Cr^{3+}	$\sim 2 \times 10^{-10}$ to $\sim 8 \times 10^{-10}$
1	nitroxyl radical	$\sim 10^{-8}$ to $\sim 10^{-6}$

III. EPR STUDIES OF ENZYMES REQUIRING SEVERAL CATIONS

Of several classes of enzymes that are known to require cations for catalytic activity, many utilize two (or more) divalent cations at or near the active site. It is well established that one of the superoxide dismutases, the Cu/Zn enzyme, has these two divalent cations in close proximity, with a bridging ligand between the ions (for recent reviews, see reference (17) and Chapter 2 of Volume 1 of Advances in Inorganic Biochemistry). Many enzymes (e.g., tyrosinase) and oxygen-carrying proteins (e.g., hemocyanin) have binuclear Cu centers as part of their native structures; recent reviews have discussed several spectroscopic features of these systems (see reference (18) and Chapter 3 of Volume 1 of Advances in Inorganic Biochemistry). It is the purpose of this section to discuss enzymes that require two or more Mg^{2+} (or Mn^{2+}) ions for full activity and to discuss spectroscopic probes to study the metal ion environment and proximity of metal ion sites on the enzyme.

At the outset we will limit ourselves to the exploration of metal ion environments by EPR spectroscopy, which cannot be used for Mg^{2+} but is feasible for several cations, such as Mn^{2+}, which usually can replace Mg^{2+} without drastically altering the activity of the enzyme. Mn^{2+} has several properties which make it easy to study for some systems and very difficult for others. It is an "S state", having one electron in each of its five d orbitals, and g is isotropic ($g_x = g_y = g_z = 2.0$) in nearly all cases. The large nuclear moment ($I = 5/2$, $A = 90G$) splits all electronic transitions into 6 lines. The electron spin relaxation time is long ($\tau_s = 10^{-9}$ to 10^{-8}s) and thus sharp lines are often observed at room temperature for enzyme-bound Mn^{2+}. However, zero-field splitting (ZFS) arising from the Kramers doublets can sometimes lead to broad featureless spectra (powder spectra) at low fields ($H_o = 3200G$, $\nu = 9$ GHz) since the $-1/2 \leftrightarrow 1/2$, $\pm 1/2 \leftrightarrow 3/2$, and $\pm 3/2 \leftrightarrow 5/2$ energy levels can all be substantially populated for large values of D and/or E. This problem can often be overcome by studies at higher field ($H_o = 12{,}200G$, $\nu = 35$ GHz), where only the $-1/2 \leftrightarrow 1/2$ transitions have a high probability of being populated. Splittings due to D and E can then be determined by computer simulation of spectra.

The spin-Hamiltonian equation for Mn^{2+} is

$$H = g\beta H_s \cdot S + D[S_z^2 - 1/3S(S + 1)] + E[S_x^2 - S_y^2] + AI \cdot S \qquad (5)$$

where D and E are the axial and rhombic components of the ZFS interaction (19). the first term is the Zeeman interaction, and $AI \cdot S$ represents interaction with nuclear spins. The ZFS interactions are anisotropic and orientation dependent. For rapidly tumbling aquo Mn^{2+} ions, D and E are averaged to zero, but for

slowly tumbling macromolecular complexes these terms do not average to zero. The net result is a "powder spectrum" with transitions spread outside the g = 2 isotropic region.

Several examples of this phenomenon have been reported (20-23), including some from our laboratory (24-26), and valuable information has been obtained concerning the environment of Mn^{2+} bound to enzymes in several complexes. Most recently the ligands bound to Mn^{2+} in an enzyme complex have been elucidated by an EPR method (27). The remainder of this article will deal with a more complex application of EPR to Mn^{2+}-enzymes, i.e., attempts to deduce the spatial relationship between the metal ions.

A. Theory of Dipolar Spin-Spin Interactions

The spin-Hamiltonian for a system of two spins can be described in general as

$$H = g\beta H\sum_i S_{iz} + \sum_{j>i}(S_i \cdot J \cdot S_j) \qquad (6)$$

where the set of spins is subjected to an external magnetic field H whose direction is taken along the Z axis. The second term embraces all interactions that are linear in spin coordinates and can be expressed as tensors. Equation 6 does not include nuclear interactions and assumes that all higher order terms $(J(S)^2)$ are negligible. The exchange terms can be of several forms representing strong coupling (or superexchange) or weak dipolar coupling. These mathematical expressions depend upon whether the spins are similar or dissimilar and whether they have different electron spin relaxation behavior. The problems associated with relating the distance between spins to the parameters observed in the spectra depend in large part on the ability to distinguish phenomena associated with the different behavior of the various forms of spin-spin interaction. We will discuss each of these next.

1. Dipolar Coupling. The classic example of a pair of superexchange-coupled paramagnetic ions is the Mn-O-Mn pair in MgO crystals doped with Mn^{2+} (28,29). The Mn-Mn separation, r_{ij}, is 2.97 Å from knowledge of the crystal lattice sites. The spin-Hamiltonian for this system is

$$H = H^i + H^j + JS^i \cdot S^j + D_e(3S_z{}^iS_z{}^j - S^i \cdot S^j) + E_e(S_x{}^iS_x{}^j - S_y{}^iS_y{}^j) \qquad (7)$$

in which $JS^i \cdot S^j$ is the isotropic part of the exchange interaction and the terms in D_e and E_e are the anisotropic terms. Evaluation of this antiferromagnetic coupling for the S = 1 state gave J = 19.5 cm^{-1}. When the transitions in the S = 1 region are fitted to the spin-Hamiltonian given in eq 5 (S = 1, g = 2),

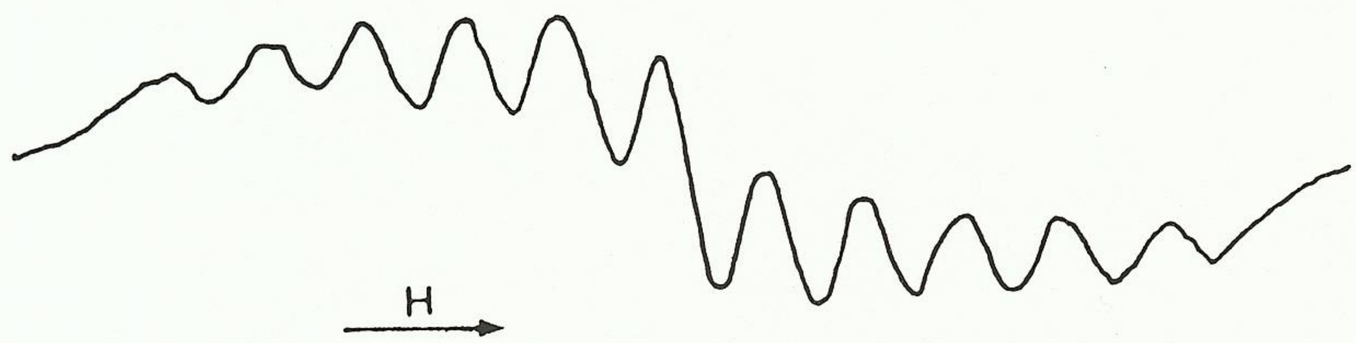

Fig. 8. EPR spectrum of part of the S = 1 region of Mn^{2+} pairs in MgO.

D = 0.776 cm^{-1} and E = 0.149 cm^{-1}. Part of the spectrum in the S = 1 region is given in Figure 8 and shows eleven lines spaced by 43 gauss as expected for strong coupling.

In an enzyme system with a well-resolved spectrum, one could estimate r if a value for D_d were obtained from fitting the spectrum. It can be shown that the axial component of eq 7 is the sum of at least two interactions with

$$D_e = D_E(\text{exchange}) + D_d(\text{dipole-dipole}) \tag{8}$$

and that

$$D_d = 111 g^2 \beta^2 / 10\ r_{ij}^{\ 3} \tag{9}$$

for a pair of Mn^{2+} ions with S =1 and S^i = 5/2 (29). For Mn^{2+} pairs doped in MgO, the calculated D_d = 0.73 cm^{-1} (using r_{ij} from crystal parameters), while the fitted value is D = 0.776 cm^{-1}. Thus the dipolar term in eq 8 dominates since the actual Mn-Mn distance might be larger. If one could extract D_d from a spectrum with a Mn^{2+} pair bound to an enzyme, an estimate of r could be obtained. Sufficient spectral resolution is often the problem in using this

TABLE V

DIPOLE-DIPOLE COUPLING CONSTANT AS A FUNCTION OF DISTANCE[a]

r (Å)	D_d	
	cm^{-1}	gauss
3	.711	7620
5	.154	1650
7	.056	600
9	.026	280
11	.014	155
13	.009	94

[a]Calculated using eq 9.

method to obtain r. Table V shows the relationship between r_{ij} and D_d using eq 9 for Mn^{2+}-Mn^{2+} pairs. In practice, if the dipole-dipole interaction were the only exchange mechanism, it would only be obvious in spectra for Mn^{2+} pairs that were <9 Å apart. This arises because a D_d value of ∿300 gauss produces an "apparent broadening" of transitions of $\lesssim$ 10 gauss due to splitting of the central -1/2 ↔ 1/2 transition. Diagrams showing the shift in line position vs. D at 9 and 35 GHz are given in a paper by Reed and Ray (30).

The problem of detecting splitting in EPR spectra of Mn^{2+} when more than one Mn^{2+} is bound is also complicated by the fact that transitions arising from each Mn^{2+} may have distinct values for D and E. Even if this complication is not apparent in the observed spectra, it must be considered for each individual system.

2. Long-Range Superexchange Interactions. Another problem recently considered by Coffman and Buettner (31,32) is whether there exists a distance-dependent limit to superexchange; in other words, over how great a distance will this coupling mechanism affect EPR spectral parameters? The superexchange mechanism is most often thought of in terms of orbital overlap between metal ions (p, d, or f orbitals) or between the metal ions and intervening ligands (p and d). Extreme orbital delocalization occurs in some crystals and produces energy bands over the entire crystal lattice. The concept of band structure is not useful when considering two metal ions bound to a macromolecule, however.

After compiling a large body of data from the literature (see Figure 1 of reference (31)), Coffman and Buettner have defined an upper limit to superexchange. They plotted log J vs. r (in Å) for antiferromagnetic and ferromagnetic substances and then considered two empirical dependencies of J on r (eqs 10 and 11).

$$J_o(R) = Ar^{-n} \tag{10}$$

$$J_o(R) = J_{oo}\exp(-\varepsilon r) \tag{11}$$

Their analysis revealed that the best-fit outer limit for expecting a contribution from superexchange follows an exponential law as in eq 11 with the numerical dependence given in eq 12.

$$J = 1.35 \times 10^7 \exp(-1.80r)\ \mathrm{cm}^{-1} \tag{12}$$

The value of ε = 1.80 holds for r > 6 Å. More extensive analysis of these equations is given in their papers. The important conclusion is that even up to

14 Å separation between spins, a small (although perhaps not measurable) amount of dipolar exchange is possible and could manifest itself as a change in line shape, reduction in signal intensity or splitting of transitions. The important practical consideration is that if spectral resolution is insufficient to detect changes in line shape or splittings, then using the above relationships is futile for determining estimates of distance between interacting ions. Notwithstanding the difficulties in observing superexchange coupling, the conclusions reached by Coffman and Buettner should always be considered in analyzing EPR data when multiple ions are bound to a macromolecule.

3. Leigh Theory of Dipolar Relaxation. The previous discussions have dealt with spin-spin exchange between pairs of like ions in crystals or bound to a macromolecule, but in several cases two dissimilar spins may be bound to a macromolecule and interact. Leigh developed a theory for the case in which two different spins bound to a rigid lattice (macromolecule) interact by dipolar spin-spin relaxation (33). When a rapidly fluctuating spin producing a magnetic field interacts with another spin, the following condition prevails

$$\delta H = \frac{g\beta\tau}{\hbar} [\langle H_z\rangle^2 + \langle H_y\rangle^2/(1 + \omega_o{}^2\tau^2)] \qquad (13)$$

in which $\langle H_z\rangle^2$ and $\langle Hy\rangle^2$ are the parallel and perpendicular components of the rapidly fluctuating field produced by the spin flips relative to the static laboratory magnetic field. Since the spins are in a rigid lattice, the correlation time (τ) describing the dipolar relaxation is identical with the T_{1e}, electron longitudinal relaxation time, of the spin producing the relaxing field. Under conditions where $\tau\omega >> 1$, the term in $\langle H_y\rangle^2$ vanishes. This condition is met for $\tau \gtrsim 10^{-11}$s at ν = 35 GHz. Equation 13 is valid for the case in which $T_{2e} > \tau$, i.e., the T_{2e} of the observed spin is greater than the T_{1e} of the perturbing spin. The net effect of dipolar relaxation is that the observed spectral lines diminish in intensity but do not broaden when the perturbing spin is present. From the line width of the observed spin one can easily calculate T_{2e} using eq 14, in which the line width (l.w.) is given in gauss.

$$(T_{2e})^{-1} = \pi g(\sqrt{3})(\text{l.w.})/7.144 \times 10^{-7} \qquad (14)$$

As stated by Leigh, if $\tau > T_{2e}$ the data can still be analyzed but the effect on the EPR spectrum is a broadening or splitting of the observed lines rather than a diminution of spectral intensity.

The reasons behind the observed diminution in line height are obvious when

one considers the following equations:

$$H_z' = \mu(1 - 3\cos^2\Theta_{R'})/r^3 \quad (15)$$

$$\delta H' = C(1 - 3\cos^2\Theta_{R'})^2 + \delta H_o \quad (16)$$

$$C = g\beta\mu^2\tau/r^6\hbar \quad (17)$$

Equation 15 describes the parallel magnetic field component at a point r from a magnetic dipole with $\Theta_{R'}$ being the angle of this dipole position vector with the magnetic field. The equation for the angularly dependent line width of the observed spin $\delta H'$ is given in eq 16 which considers the line width for all orientations $\Theta_{R'}$ of this vector in addition to the unperturbed line width δH_o. For all angles except $\Theta_{R'} \simeq 54°$, the "magic angle", the line widths are extremely broad ($\delta H \geq 1000$ G) and are unresolved, thus leading to an observed diminution in line height. For $\Theta_{R'} = 54°$, the line width is unchanged since $3\cos^2\Theta_{R'} = 1$ for this angle.

The consequences of this phenomenon can be found upon inspection of eq 17. This expression relates the relative line height remaining as a result of dipolar relaxation between spins to the distance between the spins, r. The g value corresponds to the observed spin and equals 2 in the absence of g anisotropy but more generally is equal to $(1/3)(2g_\perp + g_{||})$. The magnetic moment of the perturbing spin is $\mu^2 = S(S+1)g^2\beta^2$ and g can likewise be replaced by a more general expression if anisotropy is present, As mentioned before, $\tau = T_{1e}$ of the perturbing spin. The relationship between observed line height and $C/\delta H_o$ (normalized for the line width of the observed spin) is given in Figure 9. Thus, in practice one can easily estimate C from this plot and calculate r if T_{1e} is known. In many cases the assumption is made that $T_{1e} \simeq T_{2e}$, and T_{2e} is obtained in a separate experiment by measuring the line width. This could lead to an erroneous answer. Another method used to assess T_{1e} is to measure the frequency dependence of some ligand (H_2O for example) interacting with the enzyme-bound paramagnetic species (34).

The relationship between the relative amplitude of the line being measured and distance between spins is plotted in Figure 10 at various τ values. The range of distances between spins is a very sensitive function of τ, and some paramagnetic species are better suited than others for such studies.

Other problems associated with using this method to determine distances between paramagnetic species bound to macromolecules arise with ions that have $S > 1/2$. If these ions are used as the perturbing spin, there can be a separate

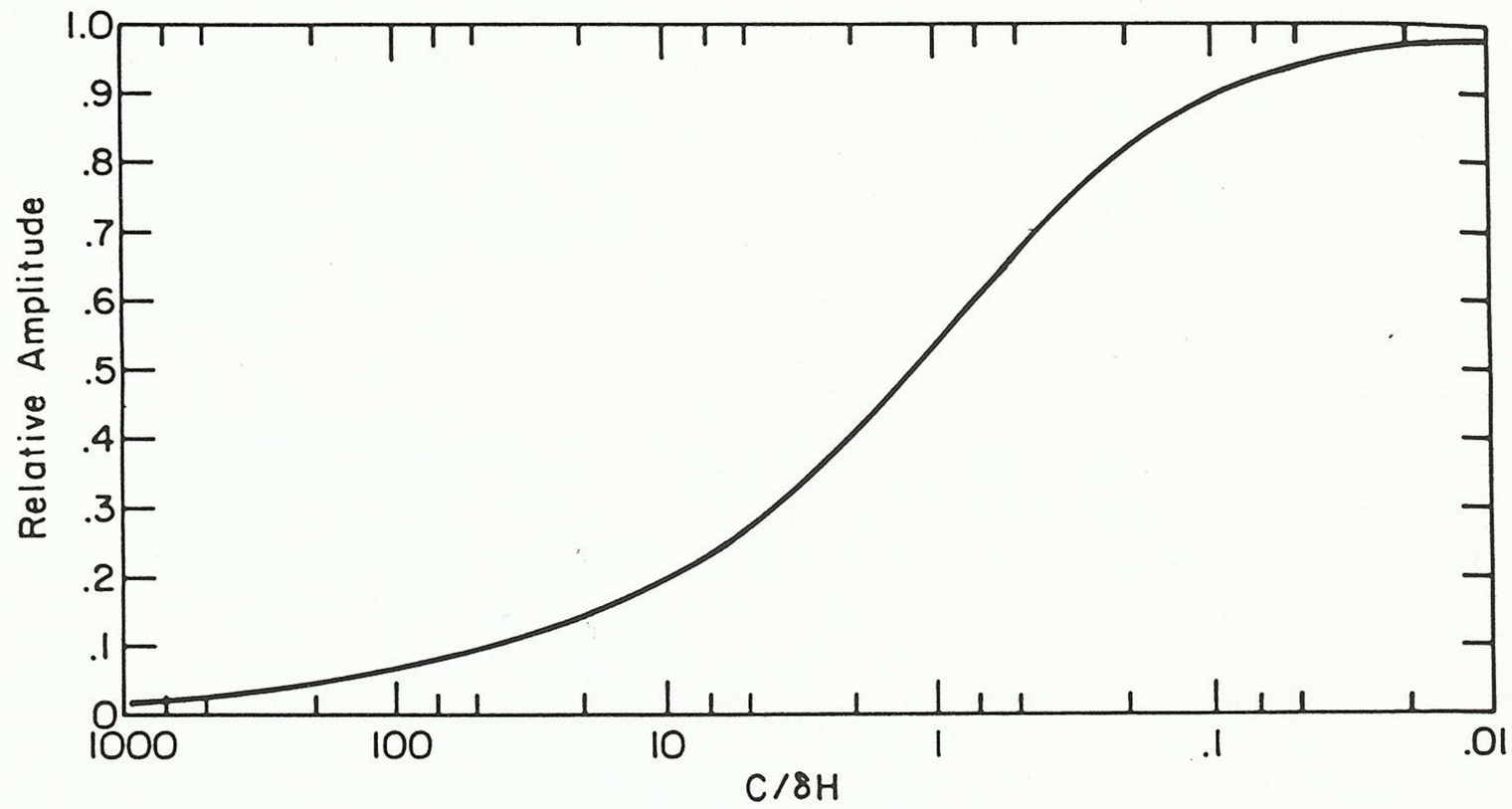

Fig. 9. Normalized amplitude of the derivative line shape for an EPR line as a function of C in eqs 16 and 17.

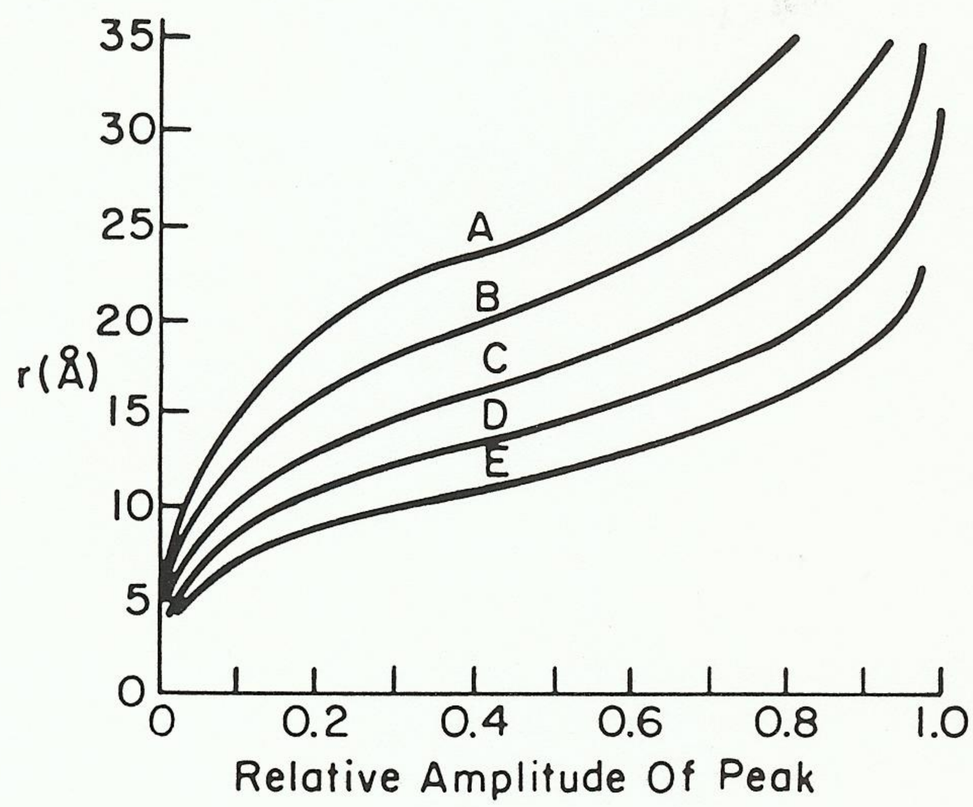

Fig. 10. Relative amplitude of an EPR line as a function of distance for the Leigh theory (eq 17) at various τ values (A-E). A, 3×10^{-8}s; B, 1×10^{-8}s; C, 3×10^{-9}s; D, 1×10^{-9}s; E, 3×10^{-10}s.

T_{1e} value for each set of transitions arising from Kramers doublets ($-1/2 \leftrightarrow 1/2$, $\pm 1/2 \leftrightarrow 3/2$, etc.). Thus an average T_{1e} may result and could invalidate the previously made assumption $T_{1e} < T_{2e}$. Also T_{1e} may be magnetic field dependent for $S > 1/2$ and would get longer at higher field; the T_{1e} would then be more than T_{2e}. Finally if the observed spin or the perturbing spin is not rigid, e.g. a "floppy" spin label, the basic premise of this theory is violated and only an upper limit to the distance will be obtained.

From the above considerations two points emerge: 1) both superexchange interactions and dipolar relaxation could be present in considering relaxation of a pair of ions (or free radicals) on the surface of a macromolecule; and 2) delineation of these various mechanisms is possible if one observes diminution in signal intensities in the absence of line broadening but only if one does not observe splitting due to the exchange mechanism. At distances <14 Å, where both mechanisms can be operating, only lower limits can safely be placed on distances from analysis by either superexchange mechanism (eqs 9 or 12).

B. Examples of Dipolar Relaxation

The Leigh theory was developed in response to an experimental observation with the enzyme creatine kinase. Upon addition of MnADP to nitroxide spin-labeled enzyme, a 95% decrease in the amplitude of the nitroxide spectrum resulted with no appreciable broadening of the spectrum (35,36). This experiment and others were evaluated using eq 17 and the following Mn-nitroxide distances were obtained : 7.5 Å with ADP and 11.5 Å with MnATP. Data were also obtained for Co^{2+} and Ni^{2+} nucleotides but were not quantitated since the condition $\omega\tau > 1$ is not met for these ions. Instead, only the qualitative assessment that C varies in the order Mn > Co > Ni was given.

An excellent review of the applications of the Leigh theory and other spin-spin interactions between nitroxides and metal ions has been published (37). This review critically assesses when dipolar relaxation theory or superexchange theory should be used to evaluate distances between paramagnetic species under many different experimental conditions. The reader is advised to consult this review as well as the papers by Coffman and Buettner when analyzing experiments involving two similar or dissimilar spins. The remainder of this article will deal with examples from our laboratory with enzymes that have two bound paramagnetic spins, most often two metal ions.

1. Glutamine Synthetase. In the past several years we have extensively studied *E. coli* glutamine synthetase because it offers the spectroscopist a wealth of metal ion, substrate, and effector binding sites with which to deter-

mine the spatial relationships. The reaction is given below:

$$\text{ATP} + \text{L-glutamate} + NH_3 \xrightleftharpoons{2M^{2+},\ M^{+}} \text{ADP} + P_i + \text{L-glutamine} \qquad (18)$$

For catalysis to occur, two divalent (and perhaps a monovalent) cation sites need to be occupied. Careful study has determined the magnitude of the binding

Fig. 11. Top: EPR spectrum of enzyme-Mn^{2+}-MSOX complex. Bottom: Same conditions as above but with saturating Cr(III)-ATP present.

constants (38-41). The enzyme is subject to covalent modification; adenylylated enzyme is activated by Mn^{2+}, while unadenylylated enzyme uses Mg^{2+} for catalysis. One metal ion site, designated the n_1 site, is a structural site which may be implicated in orienting the γ-carboxyl of glutamate, while the other metal ion (n_2 site) is established as binding to the nucleotide, ATP or ADP. Our initial studies were aimed at establishing the metal-metal internuclear distance (42, 43).

In our first report we demonstrated that the substitution-inert nucleotide Cr(III)-ATP binds competitively at the metal-ATP site. Mn^{2+} selectively binds to the n_1 site under conditions where [Enz] > [Mn^{2+}] since the K_D values for the n_1 and n_2 sites are 5×10^{-7} and 5×10^{-5} M, respectively. The signals due to bound Mn^{2+} at n_1 are representative of a relatively isotropic environment and addition of a glutamate analog, methionine sulfoximine (MSOX), produces a sharpening of the transitions and a nearly cubic geometry. When one examines the spectra at 35 GHz, the line widths of the 6 Mn^{2+} transitions are about 10G peak-to peak.

Upon addition of CrATP to enzyme-Mn-MSOX at 5°C, there is a decrease in signal amplitude of all six resonances without broadening (Figure 11). Since the T_{2e} for Mn^{2+} in this complex is 6.5×10^{-9} and the T_{1e} for Cr(III)-ATP (S = 3/2) is 2×10^{-10}s, both conditions $\omega\tau > 1$ and $T_{2e} > T_{1e}$ are met for analysis by the Leigh theory. Also, extensive examinations at lower temperatures (77 K) revealed no additional resonances for antiferromagnetically coupled Mn-Cr spins. This of course does not mean that weak superexchange does not occur, but only that is it not the dominant mechanism leading to the diminished signal intensity. Table IV summarizes several Mn-Cr distances in a number of complexes with glutamine synthetase that were obtained by the Leigh analysis of the data (43). Also included are data with Mn^{2+}- and Co^{2+}-nucleotides.

The first observation one makes from inspection of these distances is that the Mn-Cr distances are short. Using eq 9, the predicted dipole-dipole interaction for Mn^{2+} and Cr(III) at this distance is 275 gauss (for the S = 1 state for the pair and S = 3/2 for Cr(III)). This magnitude of coupling interaction should produce a slight broadening of the lines, which is not observed in the residual line (at $\Theta_{R'}$ = 54°) when dipolar relaxation is the dominant mechanism. The extent of superexchange interaction is difficult to assess since no additional transitions are observed, but a dipolar relaxation mechanism may serve to "decouple" a strong exchange mechanism in much the same way that strong H_1 fields are used to decouple spins in NMR experiments. This decoupling mechanism has not been explored in detail in systems like the ones described with glutamine synthetase.

TABLE VI

DISTANCES BETWEEN Mn^{2+} AND Cr(III) OR Co^{2+} NUCLEOTIDES FOR VARIOUS COMPLEXES OF GLUTAMINE SYNTHETASE

Enzyme Complex[a]	C[b]	r, (Å)[c]
Mn^{2+}-CrATP	30	7.1
Mn^{2+}-CrATP-glutamate	200	5.2
Mn^{2+}-CrATP-glutamate-NH_4^+	90	5.9
Mn^{2+}-CrATP-glutamine	90	5.9
Mn^{2+}-CrATP-γ-glutamyl hydroxamate	90	5.9
Mn^{2+}-CrATP-methionine(SR)-sulfoximine	40	6.8
Mn^{2+}-CrADP	90	5.9
Mn^{2+}-CrADP-P_i	200	5.2
Mn^{2+}-CrADP-glutamine	70	6.2
Mn^{2+}-CrADP-glutamine-P_i	350	4.8
Mn^{2+}-CrADP-methionine(SR)-sulfoximine	100	5.8
Mn^{2+}-CrADP-methionine(SR)-sulfoximine-P_i	20	7.6
Mn^{2+}-Co^{2+}-methionine(SR)-sulfoximine	12	7.3
Mn^{2+}-Co^{2+}-ADP-methionine(SR)-sulfoximine	25	6.5
Mn^{2+}-Co^{2+}-ADP-methionine(SR)-sulfoximine-P_i	140	4.9
Mn^{2+}-Co^{2+}-ATP-methionine(SR)-sulfoximine	90	5.2

[a]Data taken from reference (43).
[b]C was computed from the end point of a titration using Figure 9.
[c]Computed using eq 17.

The data with Co^{2+}-nucleotides and Mn^{2+} are undoubtedly underestimates of the actual distance. Since T_{1e} for Co^{2+} is in the range of 6×10^{-12}s, and since $\omega\tau \simeq 1.3$ at 35 GHz some error is introduced in the distance calculations. But since $T_{1e} >> T_{2e}$ for Mn^{2+}-Co^{2+}, it is reasonable that dipolar relaxation dominates under these experimental conditions. At low temperatures, $T < 20$ K, coupling may be observed but we have not been able to observe it at 77 K. With Co^{2+} at both sites, the EPR spectrum at 6 K does not show splitting but the resolution is quite poor, due to unresolved fine structure (43).

Since the n_2 site can be occupied by Mn^{2+} in the absence or presence of ATP, the enzyme must supply ligands to the Mn^{2+}. When ATP or ADP is present, additional phosphoryl oxygen atoms must also be ligands. From these considerations it is reasonable to suppose that when Cr(III)-nucleotides are used as analogs of MnATP, the Cr(III) does not occupy the "normal" n_2 site. We decided to study

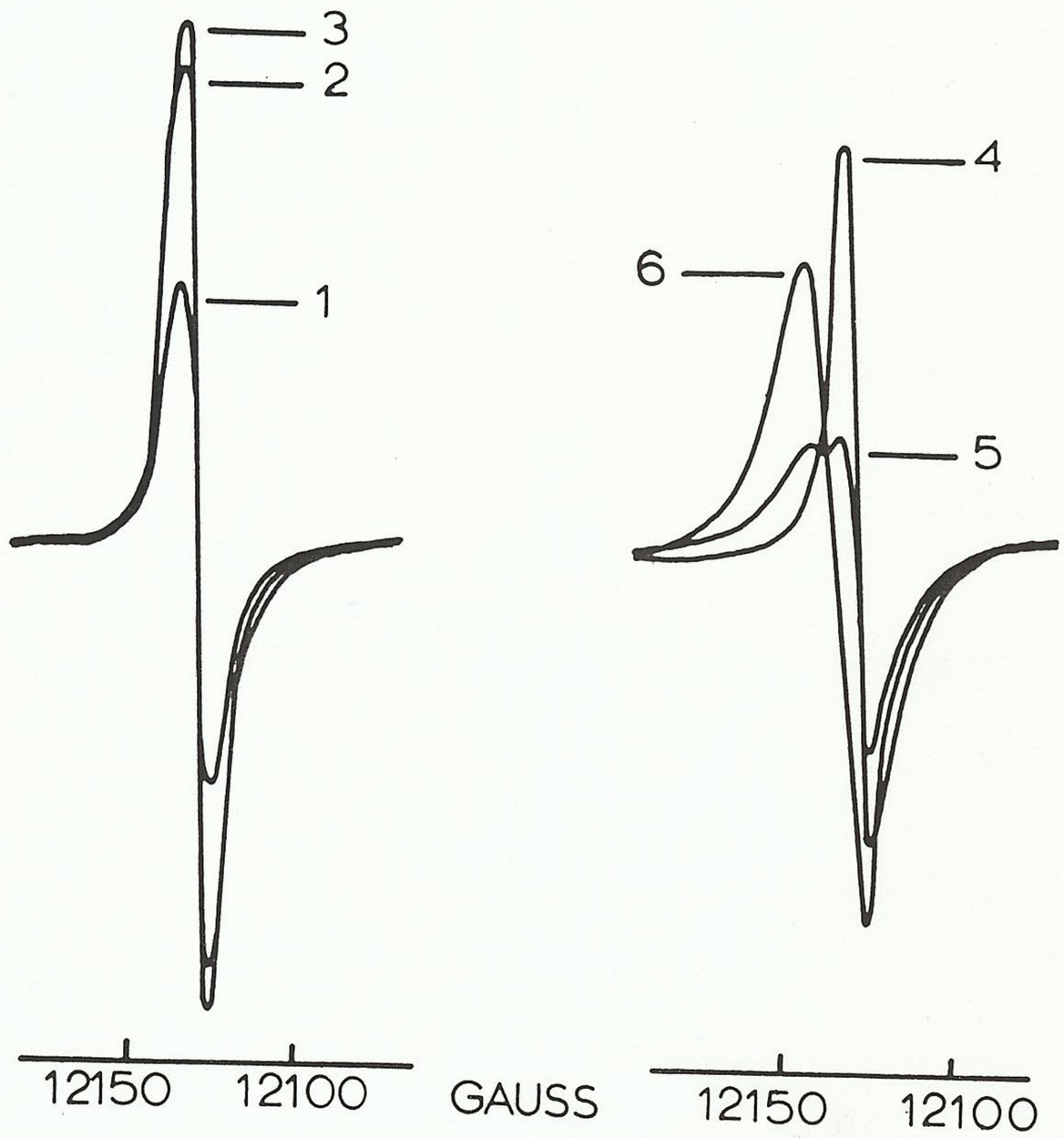

Fig. 12. Lowest field transition of the Mn^{2+} sextet in glutamine synthetase plus MSOX at various concentrations of Mn^{2+}. See Figure 13 for the full titration.

this question by adding Mn^{2+} to both sites and recording the EPR spectrum (44-46).

Figure 12 shows a single line of the six-line spectrum of enzyme with MSOX as Mn^{2+} is added. Numbers 1-3 represent successive additions of Mn^{2+} up to one Mn^{2+} (n_1 site) per subunit. When more Mn^{2+} is added to occupy the n_2 site, the spectra numbered 4-6 are obtained. A full set of data is shown in Figure 13. The observation is that as the n_2 site is occupied with Mn^{2+}, the spectrum of Mn^{2+} at n_1 <u>decreases</u>. Separate experiments show that when Mg^{2+} is at n_1, the spectrum of Mn^{2+} is split into several transitions due to a large ZFS. Thus, the spectrum due to Mn^{2+} at n_2 is "spread out" and these transitions are not seen at the same gain settings used to observe the quite sharp Mn^{2+} lines when MSOX is present. The decrease in Mn^{2+} signal at n_1 as Mn^{2+} occupies n_2 is

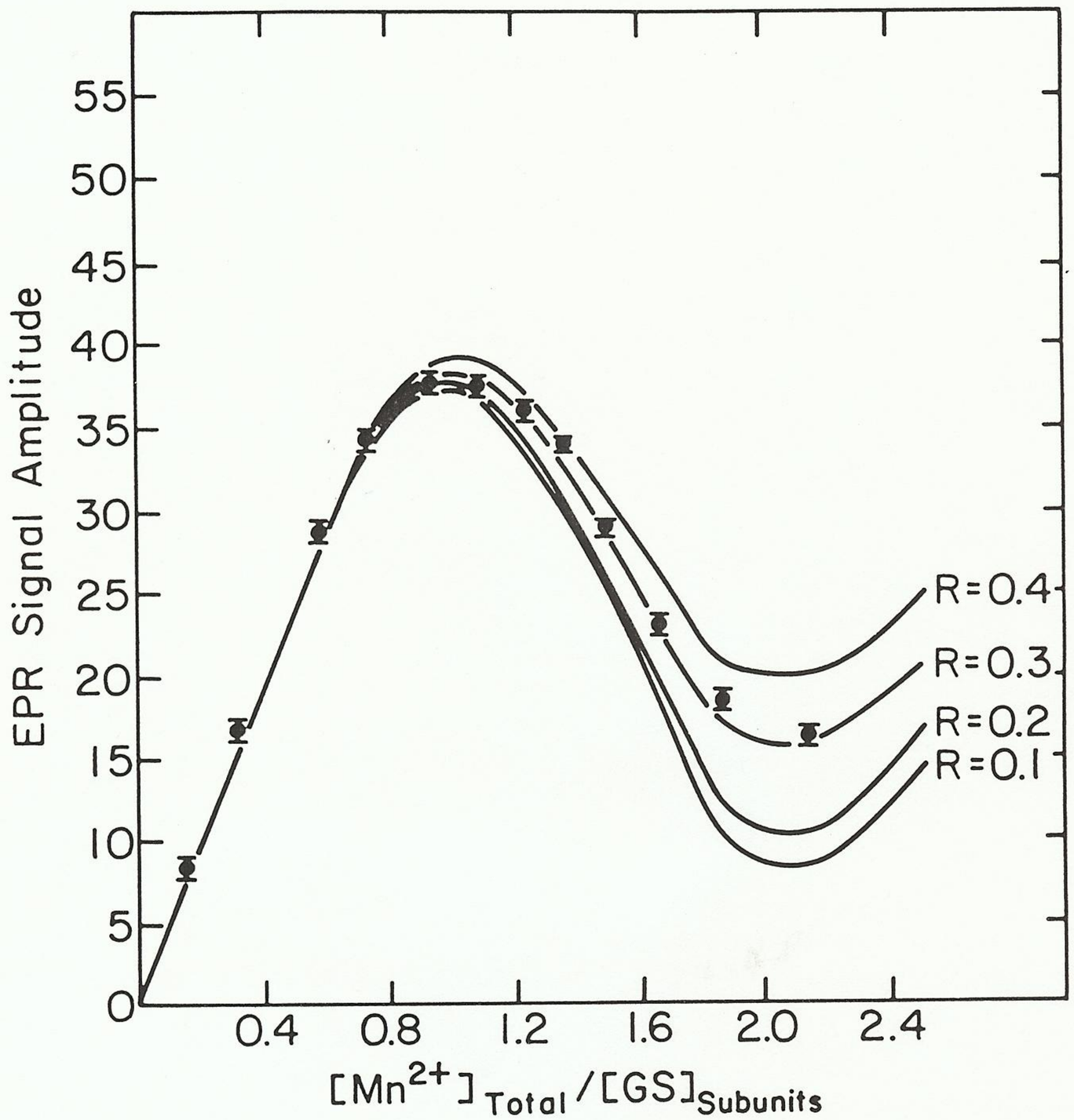

Fig. 13. Titration of glutamine synthetase plus MSOX with Mn^{2+}. R is defined in Table VII.

therefore due to superexchange coupling or dipolar relaxation or both.

We could not observe the coupled spectra due to Mn-Mn pairs at 9 and 35 GHz at 77 K. We conclude that dipolar relaxation is a dominant mechanism producing the diminished, but not broadened Mn^{2+} spectrum at n_1 and we observe that T_{1e} (by NMR) of Mn^{2+} at n_2 is greater than T_{2e} of Mn^{2+} at n_1. Spectrum number 5 (Figure 12) shows both bound Mn^{2+} and free Mn^{2+}, and spectrum 6 shows mostly free Mn^{2+} as the Mn^{2+} concentration exceeds 2 Mn^{2+} per subunit.

Using these findings we tried to fit the data to an expression for extrapolating and determining the amplitude of the Mn^{2+} spectrum at n_1 when Mn^{2+} is saturating at n_2. The curves in Figure 13 were determined by computer fit to

TABLE VII

ANALYSIS OF EPR DATA FOR GLUTAMINE SYNTHETASE

Complex[a]	C	R[b]	r (Å)
Mn_2-GS-Mn_1-MSOX	28.5-57.0	0.35-0.25	11.5-13
Mn_2-ADP-P_i-GS-Mn_1-MSOX	57- 166	0.15-0.25	10.2-12.2
Mn_2-(AMP-PNP)-GS-Mn_1-MSOX	77- 667	0.08-0.22	8.1-11.2

[a]The subscripts 1 and 2 refer to Mn at sites n_1 and n_2, respectively.
[b]The data were analyzed by the following expression:

$$I = \varepsilon_1[E_1] + \varepsilon_1[E_{12}](1-R) + \varepsilon_2[Mn]$$

where I is the total signal height; ε_1 is the maximum intensity of Mn^{2+} at the n_1 site: ε_2 is that for free Mn^{2+}; E_1 and E_{12} are enzyme species with one and two Mn^{2+}, respectively; and R is the reduction of Mn^{2+} intensity at n_1 produced by Mn^{2+} bound at n_2 (44).

the data. Table VII shows the fit of the data using eq 17. The T_{1e} of Mn^{2+} at n_2 is 2×10^{-9}s, as determined by frequency-dependent NMR studies of the proton relaxation rate of H_2O interacting with enzyme-bound Mn^{2+}. Thus T_{2e} for Mn^{2+} at n_2 is greater than T_{1e} for Mn^{2+} at n_1. The Mn^{2+}-Mn^{2+} distances are ∿8-11 Å in the presence of nucleotides. In this range, weak superexchange could still be expected according to Coffman and Buettner but the magnitude of J would be small, <0.01 cm^{-1}, and might produce only a slight broadening in the Mn^{2+} spectra and thus elude detection. With a limit for superexchange of ∿14 Å, this mechanism is expected to be present but insignificant for this system.

On the basis of the analysis above, we conclude that the Cr(III) nucleotides bind at the nucleotide site but that Cr(III) is displaced from the "true" n_2 metal ion site, as shown in Figure 14. Although this conclusion is based on the validity of the data analysis for the EPR spectra using the theories outlined, from the arguments presented the data analysis represents good estimates of metal-metal distances for glutamine synthetase complexes.

2. Inorganic Pyrophosphatase. Yeast inorganic pyrophosphatase catalyzes the following reaction:

$$PP_i + H_2O \xrightarrow{?M^{2+}} 2P_i \qquad (19)$$

This simple reaction has a complex dependency on metal ion concentration, and it has been suggested that up to three metal ions are involved in catalysis (47-51).

In collaboration with Dr. Dunaway-Mariano, we studied Mn^{2+} binding to this enzyme with EPR by the same method used for glutamine synthetase. A titration

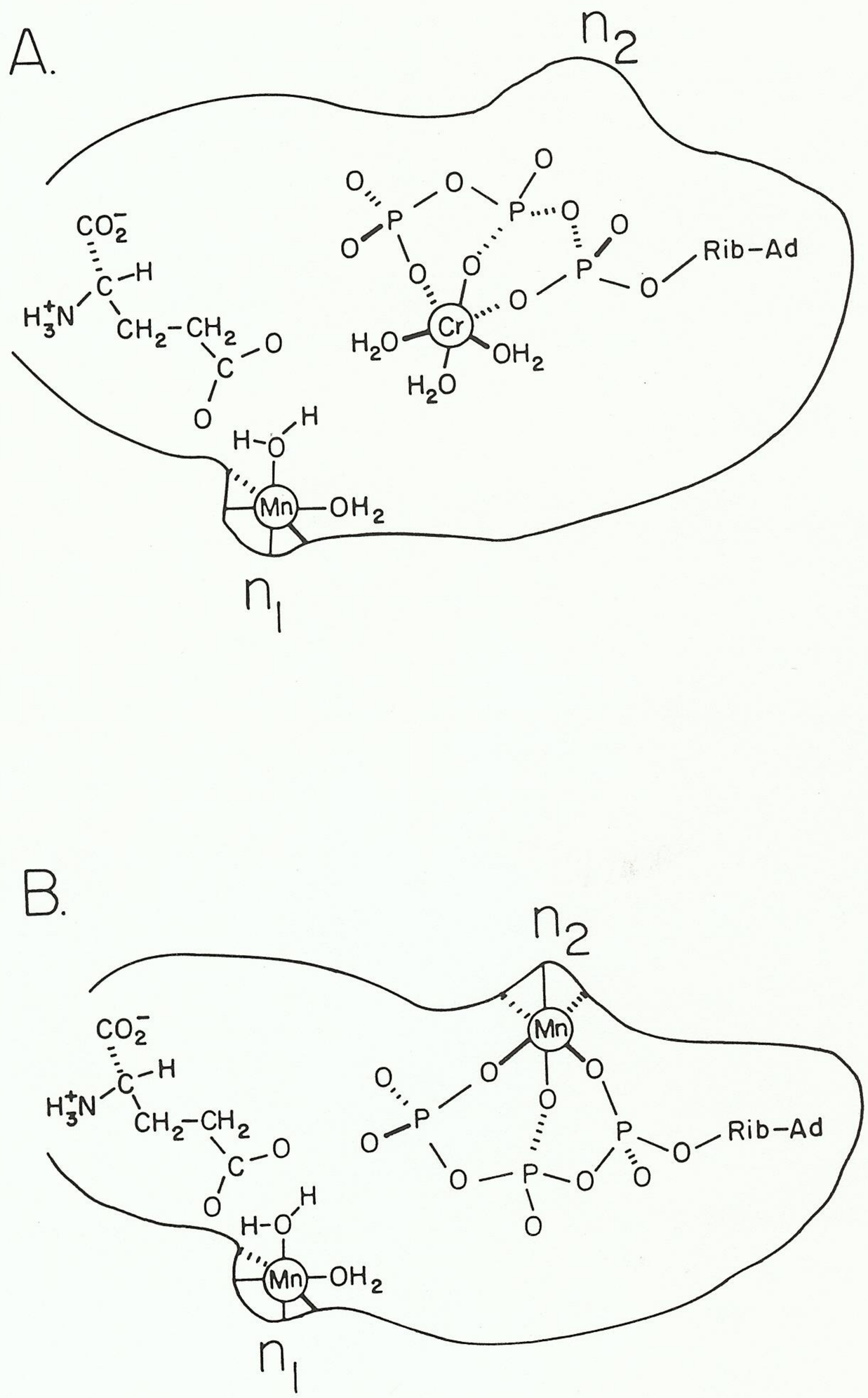

Fig. 14. Schematic representation of the active site of glutamine synthetase A, with Cr(III)-ATP and B, with Mn^{2+}-ATP at the n_2 metal-nucleotide site.

of pyrophosphatase with Mn^{2+} is shown in Figure 15. It is clear that at least two Mn^{2+} bind and that the two metal ions interact since the total intensity of the Mn^{2+} signal diminishes above one Mn^{2+} per subunit until free Mn^{2+} is seen. Currently we do not have an EPR spectrum of Mn^{2+} at the second site, but analysis of proton NMR data of H_2O as a function of frequency is consistent with slightly different T_{1e} and T_{2e} values for the two Mn^{2+}. Analysis by eq 17 reveals a Mn^{2+}-Mn^{2+} estimate of 10-12 Å, but further refinement of the data is obviously necessary.

Figure 15 also shows the Mn^{2+} titration in the presence of the diamagnetic substrate analog $Co(III)(NH_3)_4(PNP)$ and the paramagnetic $Cr(III)(NH_3)_4(PNP)$ analog. When Cr(III) is present, the total intensity diminishes substantially, in-

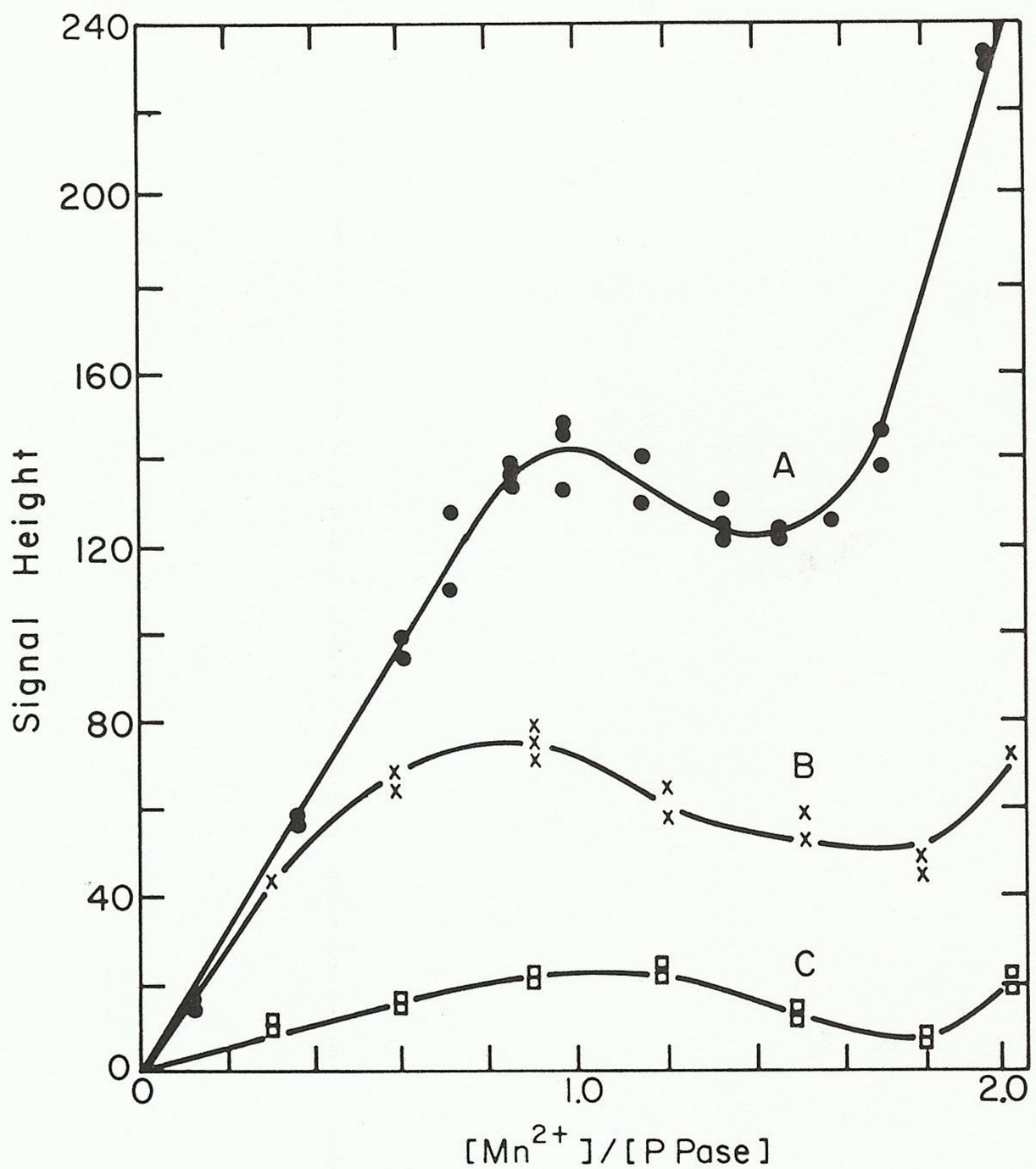

Fig. 15. Titration of pyrophosphatase with Mn^{2+}. A, enzyme alone; B, enzyme plus $Co(III)(NH_3)_4(PNP)$: C, enzyme plus $Cr(III)(NH_3)_4(PNP)$.

dicating interaction among Cr(III) and the two bound Mn^{2+}. These ions must be in close proximity (6-10 Å) but analysis of the data by eqs 9, 12, or 17 is not possible for this 3-spin system. Other experiments may reveal separate interactions in this complex enzyme.

IV. CONCLUSIONS

Two different methods have been discussed in this review to study spatial relationships in enzymes that have several metal ions involved in catalysis. Both the NMR and EPR methods described in this paper are applicable to many very complex enzymes. It is our hope that this review will stimulate further study with simple and complex enzymes in ways that will reveal how monovalent and divalent cations participate in enzymic catalysis.

REFERENCES

1. C.H. Suelter, Science, 168, 789 (1970).
2. R.K. Gupta and A.S. Mildvan, J. Biol. Chem., 252, 5967 (1977).
3. A.S. Mildvan, D.L. Sloan, C.H. Fung, R.K. Gupta, and E. Melamud, J. Biol. Chem., 251, 2431 (1976).
4. H.G. Hertz, Ber. Bunsenges. Phys. Chem., 77, 531 (1973).
5. B. Lindman and S. Forsén in "NMR and the Periodic Table", R.K. Harris and B.E. Mann, Eds., Academic Press, London, 1978, pp 129-181.
6. F.J. Kayne in "The Enzymes", P.D. Boyer, Ed., Academic Press, New York, 1973, pp 353-372
7. T. Nowak, J. Biol. Chem., 248, 7191 (1973).
8. T. Nowak, J. Biol. Chem., 251, 73 (1976).
9. J. Reuben and F.J. Kayne, J. Biol. Chem., 246, 6227 (1971).
10. W.E. Hutton, E.E. Stephens and C.M. Grisham, Arch. Biochem. Biophys., 184, 166 (1977).
11. D.E. Ash, F.J. Kayne and G.M. Reed, Arch. Biochem. Biophys., 190, 571 (1978).
12. G.H. Reed and M. Cohn, J. Biol. Chem., 248, 6436 (1973).
13. F.M. Raushel and J.J. Villafranca, Biochemistry, 19, 5481 (1980).
14. R.A. Dwek, "Nuclear Magnetic Resonance in Biochemistry", Clarendon Press, Oxford, 1973.
15. F.M. Raushel and J.J. Villafranca, J. Am. Chem. Soc., 102, 6618 (1980).
16. F.M. Raushel, C.J. Rawding, P.M. Anderson, and J.J. Villafranca, Biochemistry, 18, 5562 (1979).
17. J.S. Valentine and M.W. Pantoliano in "Copper Proteins", T.G. Spiro, Ed., Wiley-Interscience, John Wiley & Sons, New York, 1981, pp 291-358.
18. E.I. Solomon in "Copper Proteins", T.G. Spiro, Ed., Wiley-Interscience, John Wiley & Sons, New York, 1981, pp 41-108.
19. A. Abragam and B. Bleaney, "Electron Paramagnetic Resonance of Transition Ions", Oxford Univ. Press (Clarendon), London, 1970.
20. G.H. Reed and M. Cohn, J. Biol. Chem., 247, 3072 (1972).
21. G. Michaels, Y. Milner, and G.H. Reed, Biochemistry, 14, 3213 (1975).
22. D.H. Buttlaire, G.H. Reed and R.H. Himes, J. Biol. Chem., 250, 261 (1975).
23. R.E. Weiner, J.F. Chlebowski, P.H. Haffner and J.E. Coleman, J. Biol. Chem., 254, 9739 (1979).
24. J.J. Villafranca, D.E. Ash and F.C. Wedler, Biochemistry, 15, 544 (1976).
25. R.S. Levy and J.J. Villafranca, Biochemistry, 16, 3293 (1977).
26. J.J. Villafranca and F.M. Raushel, Adv. Catalysis, 28, 323 (1979).

27. G.H. Reed and T.S. Leyh, Biochemistry, 19, 5472 (1980).
28. B.A. Coles, J.W. Orton and J. Owen, Phys. Rev. Lett., 4, 116 (1960).
29. J. Owen, J. Appl. Phys. Suppl., 32, 213S (1961).
30. G.H. Reed and W.J. Ray, Jr., Biochemistry, 10, 3190 (1970).
31. R.E. Coffman and G.R. Buettner, J. Phys. Chem., 83, 2387 (1979).
32. R.E. Coffman and G.R. Buettner, J. Phys. Chem., 83, 2392 (1979).
33. J.S. Leigh, Jr., J. Chem. Phys., 52, 2608 (1970).
34. R.A. Dwek, "NMR and Biochemistry", Oxford Univ. Press (Clarendon), London, 1973.
35. J.S. Taylor, J.S. Leigh, Jr., and M. Cohn, Proc. Natl. Acad. Sci. U.S.A., 64, 219 (1969).
36. M. Cohn,H. Diefenbach and J.S. Taylor, J. Biol. Chem., 246, 6037 (1971).
37. S.S. Eaton and G.R. Eaton, Coord. Chem. Rev., 26, 207 (1978).
38. A. Ginsburg, Advan. Prot. Chem., 27, 1 (1972).
39. J.B. Hunt, P.Z. Smyrniotis, A. Ginsburg and E. Stadtman, Arch. Biochem. Biophys., 166, 102 (1975).
40. J.J. Villafranca and F.C. Wedler, Biochemistry, 13, 3286 (1974).
41. J.J. Villafranca, D.E. Ash, and F.C. Wedler, Biochemistry, 15, 536 (1976).
42. J.J. Villafranca, M.S. Balakrishnan, and F.C. Wedler, Biochem. Biophys. Res. Commun., 75, 464 (1977).
43. M.S. Balakrishnan and J.J. Villafranca, Biochemistry, 17, 3531 (1978).
44. E.J. Gibbs, M.S. Thesis, The Pennsylvania State University, 1980.
45. E.G. Spiro, S. Ransom, Fed. Proc., 39, Abstr. 1326 (1980).
46. S. Ransom, E.J. Gibbs, and J.J. Villafranca, manuscript in preparation.
47. W.B. Knight, S.W. Fitts and D. Dunaway-Mariano, Biochemistry, 20, 4079 (1981).
48. B.S. Cooperman, A. Panackal, B. Springs, and D.J. Hamm, Biochemistry, 20, 6051 (1981).
49. B. Springs, K.M. Welsh, and B.S. Cooperman, Biochemistry, 20, 6384 (1981).
50. W.B. Knight, D. Dunaway-Mariano, and J.J. Villafranca, Fed. Proc., 41, Abstr. 3732 (1982).
51. K.M. Welsh, I.M. Armitage, and B.S. Cooperman, Fed. Proc., 41, Abstr. 3736 (1982).